

# Quasicrystal–crystal structural transformation in Al–5 wt.% Mn alloy

Karel Saksl · Dalibor Vojtěch · Hermann Franz

Received: 24 January 2006 / Accepted: 11 December 2006 / Published online: 10 May 2007  
© Springer Science+Business Media, LLC 2007

**Abstract** The atomic structure of Al–5 wt.%Mn (Al–5Mn) alloy, prepared by rapid solidification, and pre-annealed at 623 and 773 K for 5 and 1 h, respectively, were characterized by X-ray powder diffraction (XRD) and extended X-ray absorption fine structure (EXAFS) techniques. The sample in as-quenched stage was found crystalline, consisting of metastable  $\alpha$ -Al (Al–Mn solid solution) and icosahedral quasicrystalline I-Al<sub>6</sub>Mn phases. Five hours annealing at 623 K proved thermal stability of both the phases. Pre-annealing at 773 K/1 h on the other hand leads to  $\alpha$ -Al phase decomposition and structural transformation of metastable I-Al<sub>6</sub>Mn to stable orthorhombic Al<sub>6</sub>Mn phase. The EXAFS results indicate that Mn atoms are located preferably on the outer shell of icosahedrons. During the I-Al<sub>6</sub>Mn  $\rightarrow$  o-Al<sub>6</sub>Mn transformation the total Al atoms coordinating one Mn were found to be constant (~10). Based on the results, only distance/symmetry changes in atomic arrangement around Mn atoms were suggested.

## Introduction

Rapid solidification (RS) processing has the potential for substantial improvements of mechanical properties through

---

K. Saksl (✉) · H. Franz  
HASLAB am Deutschen Elektronen Synchrotron, DESY,  
Notkestrasse 85, 22603 Hamburg, Germany  
e-mail: karel.saksl@desy.de

K. Saksl  
Institute of Materials Research, Slovak Academy of Sciences,  
Watsonova 47, 043 53 Kosice, Slovak republic

D. Vojtěch  
Department of Metals and Corrosion Engineering,  
Institute of Chemical Technology, Technická 5, 16628 Prague 6,  
Czech Republic

the extension of solid solubility limits, the refinement of microstructure, and dispersion of the secondary phases. Furthermore, by this method it is possible to produce metastable phases such as quasi-crystals, nano-crystals, and amorphous whose presence in an alloy leads to beneficial improvements in mechanical, magnetic, electrical, and other properties. Al–Mn is an important system in which the occurrence of a quasicrystalline non-equilibrium phase was discovered [1]. Since this discovery, various Al–Mn–X (X = Si, Be, Pd, Fe, Cr, Ni, Y, La, Nd, Gd etc.) alloys have been investigated in detail [2–8]. However, relatively little information are available about the structural evolution of the RS Al–Mn based alloys upon heating. In this paper we present our structural study on Al–5 wt.% Mn (Al–5Mn) alloy prepared by melt-quenching and after annealing at selected temperatures. The atomic structures of subjected samples were examined by X-ray powder diffraction (XRD) and extended X-ray absorption fine structure (EXAFS) techniques.

## Experimental

Ingot, with nominal composition Al–5 wt.%Mn (Al–5Mn) was prepared by melting a mixture of pure Al (99.99%) and Mn (99.99%) in resistance furnace in argon atmosphere. A 50  $\mu$ m-thick and 7 mm wide ribbon sample was obtained from this master alloy ingot by single rolled melt spinning at a wheel surface velocity of 40 m/s. In order to investigate the structure of the alloy after annealing at high temperatures two sets of samples were pre-annealed at 623 and 773 K for 5 and 1 h, respectively, in argon.

High energy X-ray powder diffraction measurements were performed at HASLAB at DESY (Hamburg, Germany) on the experimental station BW5 [9] using

monochromatic synchrotron radiation of 79 keV ( $\lambda = 0.1573 \text{ \AA}$ ). The samples measured at room temperature in transmission mode were illuminated for 120 s by a well collimated incident beam of  $0.5 \text{ mm}^2$  cross-section. The XRD patterns were recorded by a 2D detector (mar345 Image plate) in asymmetric mode. The background intensity was subtracted directly from the 2D XRD pattern and the result was integrated to 2 Theta space by using the program Fit2D [10]. The diffractometer parameters such as: sample detector distance, detector orthogonality with respect to the incoming radiation, precise radiation energy was determined by comparing a standard reference LaB<sub>6</sub> sample [11].

The Mn-K edge EXAFS measurements were performed at HASYLAB at beamline A1. Spectra were collected in transmission mode using the fixed exit Si(111) channel cut monochromator. The X-ray intensities were monitored using ionization chambers filled by N<sub>2</sub> the pressure of which was adjusted to the scanned photon energy range. The energy calibration was monitored using reference materials measured together with the sample. Experimentally measured X-ray absorption cross sections  $\mu(E)x$  were analysed by standard procedures of data reduction, using the program Viper [12]. First the EXAFS signal,  $\chi(k)$  was extracted and weighted by  $k^3$  and a Kaiser-Bessel apodization function (coefficients  $A = 12$ ,  $\bar{k}=7$ ), followed by Fourier transformation (FT) over the region where the amplitude of the non-weighted  $\chi(k)$  is significant (for details see [12]). The FT gives a radial distribution function (RDF), modified by the phase shifts due to the absorbing and backscattering atoms. The contribution of the first shells only was backtransformed into k-space. The structural parameters N (coordination number), R (interatomic distance), and  $\sigma^2$  (mean-square relative displacement) were obtained from least squares fitting in k-space, using theoretical phases and amplitude functions calculated by the FEFF-8 code [13].

## Results and discussion

### XRD measurements

Figure 1 shows XRD patterns of as-quenched Al-5Mn sample and the same alloy pre-annealing at different temperatures. The sample in as-quenched stage and after pre-annealing at 623 K/5 h shows similar patterns consisting of dominant fcc  $\alpha$ -Al Bragg's peaks (marked by asterisk) and low intensity reflections originating from metastable icosahedral quasicrystalline I-Al<sub>6</sub>Mn (PDF No.390952, open triangles). The sample pre-annealed at 773 K/1 h unlike the previous, consists of fcc-Al and an orthorhombic Al<sub>6</sub>Mn (PDF No.411285) phases. The schematic drawing

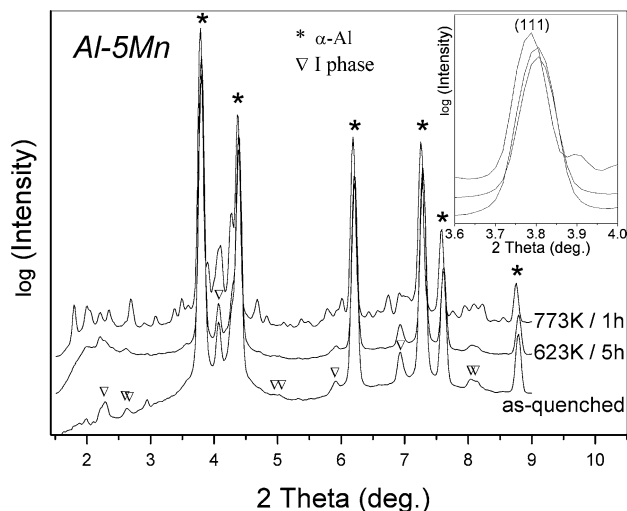


**Fig. 1** XRD patterns of Al-5Mn sample in as-quenched stage and after pre-annealing at 623 K/5 h and 773 K/1 h with marked positions of  $\alpha$ -Al and quasicrystalline I-Al<sub>6</sub>Mn peaks. The insert shows a shift of strongest reflection Al (111) after pre-annealing at 773 K/1 h

of all the phases is shown on Fig. 2. Another noticeable feature resulting from visual examination of the XRD patterns is a pronounced shift of  $\alpha$ -Al peaks towards lower 2 Theta angles observed on sample pre-annealed at 773 K/1 h (see also the figure insert). Such a peaks position displacement reflects a change (increase) of the fcc lattice parameter, quantification of which was addressed to Rietveld refinement. The obtained  $\alpha$ -Al lattice parameters for as-quenched, pre-annealed at 623 K/5 h and 773 K/1 h samples were found to be 4.04, 4.038 and 4.05  $\text{\AA}$ , respectively. Comparing these values to 4.049  $\text{\AA}$  (reported for pure Al) brought us to the conclusion that the primary  $\alpha$ -Al phase is a supersaturated solid solution of Mn atoms in the Al lattice. An existence of solid solution phase in alloy is not surprising taking into account the sample was prepared by rapid solidification process. Similarly, the lattice parameter reduction can satisfactorily be explained by the difference of nominal atomic radii between Mn (1.26  $\text{\AA}$ ) and Al (1.43  $\text{\AA}$ ) [14]. Substitutional alloying of Al fcc lattice by smaller Mn atoms results in  $\alpha$ -Al lattice volume shrinking. The identified solid solution phase exhibits in addition a high thermal stability extending over 623 K annealing for 5 h. Further annealing at 773 K for 1 h transforms the quasicrystalline I-Al<sub>6</sub>Mn fraction to the more stable *o*-Al<sub>6</sub>Mn and decomposes the solid solution into *o*-Al<sub>6</sub>Mn and purified fcc-Al phases.

### EXAFS measurements

The normalized and  $k^3$  weighted EXAFS data of as-prepared and pre-annealed Al-5Mn alloy measured above the Mn K-edge are displayed in Fig. 3a. Oscillatory signals

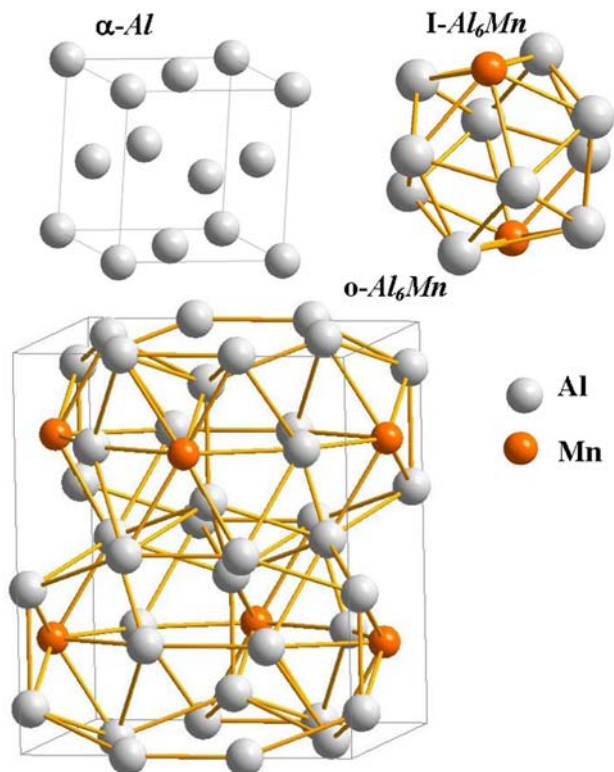
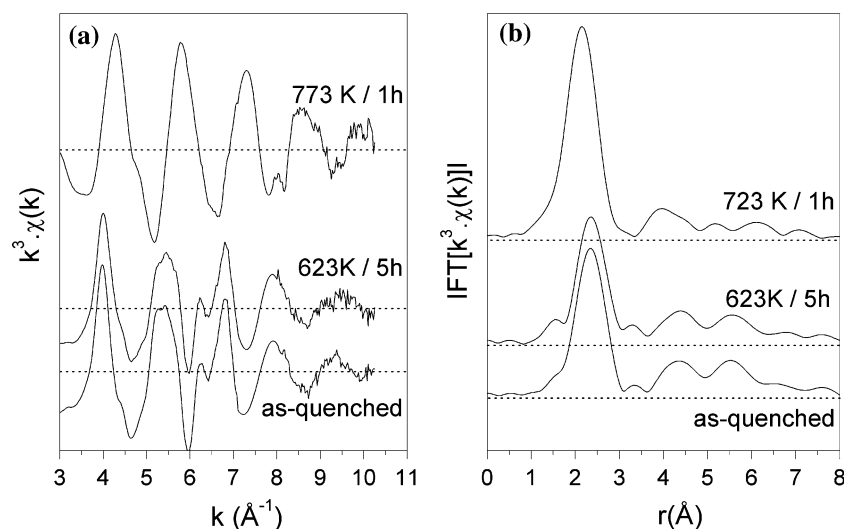


**Fig. 2** Schematic drawing of fcc-Al (S.G.:  $Fm\bar{3}m$ ,  $a = 4.049 \text{ \AA}$ ), quasicrystalline  $I\text{-Al}_6\text{Mn}$ , and orthorhombic  $\text{Al}_6\text{Mn}$  (S.G.:  $Cmcm$ ;  $a = 7.555 \text{ \AA}$ ,  $b = 6.499 \text{ \AA}$ ,  $c = 8.872 \text{ \AA}$ ) phases

taken from as-prepared and pre-annealed at 623 K/5 h samples look similar while the last annealing step to 773 K/1 h changes the signal significantly. Corresponding Fourier transforms of  $k^3 \cdot \chi(k)$  to  $r$ -space, Fig. 3b, show distinct shifts of the main peak from  $\sim 2.3$  to  $\sim 2 \text{ \AA}$  of the sample pre-annealed at 773 K. These observations in the local atomic arrangements around Mn are presumably

**Fig. 3** Experimental  $k^3 \cdot \chi(k)$  of Al–5Mn alloy in as-quenched stage and after pre-annealing at 623 K/5 h and 773 K/1 h measured above the Mn–K edge, b. corresponding Fourier transforms



consequence of the formation of the stable orthorhombic  $\text{AlMn}_6$  phase, documented also by the XRD experiments.

In order to obtain quantitative values for the structural parameters  $R$ ,  $N$  and  $\sigma^2$  numerical fitting of the BFT signals was performed with  $S_0^2$  constrained to the value suggested by FEFF ab-initio theoretical calculation. Results of these numerical fits are listed in Table 1 and the comparisons of filtered and calculated EXAFS spectra are shown on Fig. 4. From the local atomic structure refinement follows that the total number of Al coordinating one Mn atom in average is  $\sim 10$ , regardless of annealing, while the Mn–Al interatomic distance decrease significantly (7%) after pre-annealing at 773 K. Similarly, the value of the mean-square displacement significantly decreases after high temperature annealing. One can therefore assume exclusive distance/symmetry changes in local atomic arrangements around the Mn. Let us now have a closer look to the atomic arrangement of the icosahedral quasicrystalline phase. In icosahedrons atoms might sit either on the outer shell (top of the pentagon cups) or in centre of the body. The atom located in the centre of icosahedron body is coordinate by 12 while the atom sitting on the top of the pentagon cups is coordinate by 10 nearest neighbours. The coordination numbers extracted from EXAFS signal analysis is 10, therefore one can assume that Mn atoms sits on the shell of icosahedron. The local atomic order around Mn atoms in the icosahedral phase and after transformation to the stable orthorhombic phase is shown on Fig. 5. On the picture, the total numbers of Al atoms remains constant, while only the symmetry and average interatomic distance of Al atoms changes.

## Conclusions

In this work we present our structural study upon Al–5 wt.% Mn alloy prepared by rapid solidification and after

**Table 1** Structural parameters of Al-5Mn alloy determined from the Mn-K edge EXAFS spectra. C and B mean central and back-scattering atom, respectively

Annealing [K/h]	C-B pairs	$R$ (Å)	$N$	$\sigma^2$ (Å <sup>2</sup> )
As prepared	Mn–Al	$2.764 \pm 0.005$	$10.8 \pm 0.5$	$0.0171 \pm 0.0007$
623/5	Mn–Al	$2.765 \pm 0.006$	$9 \pm 0.8$	$0.0173 \pm 0.0014$
773/1	Mn–Al	$2.562 \pm 0.006$	$10.4 \pm 0.6$	$0.0137 \pm 0.0009$

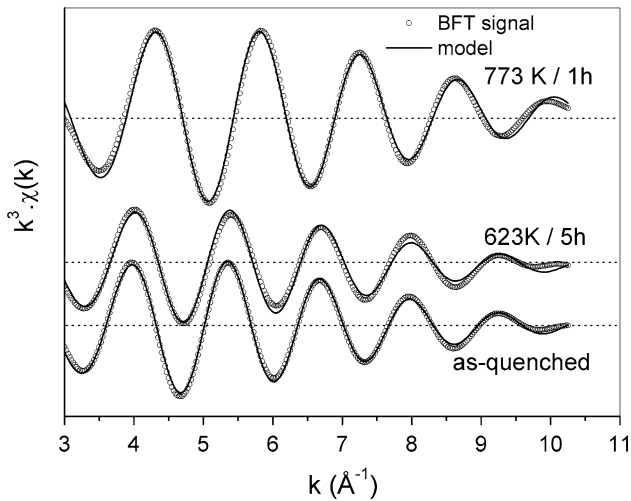


**Fig. 4** Comparison of filtered and calculated fit of Mn–K edge EXAFS data using structural data listed in Table 1

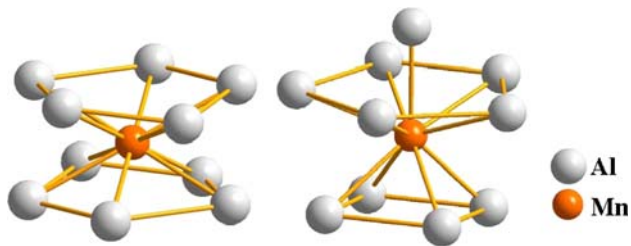


**Fig. 5** Local atomic order (first coordination shell) around the Mn atom in the icosahedral phase (left) and in orthorhombic Al<sub>6</sub>Mn phase (right)

pre-annealing at 623 and 773 K for 5 and 1 h, respectively. The atomic structures of all samples were characterized by XRD and EXAFS techniques. The sample in as-quenched stage was found crystalline having only a small fraction of glassy phase. The lack of amorphous phase is likely caused by insufficient cooling rate during the melt quenching process. The XRD patterns from the as-quenched sample and the sample after pre-annealing at 623 K/5 h samples showed presence of:  $\alpha$ -Al (Al–Mn solid solution) and icosahedral quasicrystalline I-Al<sub>6</sub>Mn phases in the alloy. The existence of primary Al–Mn solid solution in the alloy prepared by rapid quenching was confirmed. The lattice parameter of  $\alpha$ -Al is about 3% smaller than parameter

reported for pure Al phase. Such a reduction can satisfactorily be explained by substitutional alloying Al matrix by smaller Mn atoms. Pre-annealing at 773 K on the other hand leads to decomposition of  $\alpha$ -Al phase, transformation of metastable I-Al<sub>6</sub>Mn to stable orthorhombic Al<sub>6</sub>Mn phase and purified fcc-Al phase.

The EXAFS signal analysis demonstrates a similar local atomic arrangement around Mn in as-quenched sample and after pre-annealing at 623 K/5 h. The icosahedral quasicrystalline phase has presumably the Mn atoms located at the outer shell (top of the pentagons cups) rather than in the center of icosahedron body. Pre-annealing to 773 K further leads to significant Mn–Al interatomic distance shortening (7%) coupled with  $\sigma^2$  reduction reflecting the formation of the stable and more confined orthorhombic phase. During the EXAFS analysis we found interesting that the total Al atoms coordinating one Mn atom remains constant (~10) for all samples. Following the over-all picture of I-Al<sub>6</sub>Mn  $\rightarrow$   $\alpha$ -Al<sub>6</sub>Mn transformation, we predict only the distance/symmetry changes of closest Al neighbours around the Mn atoms.

**References**

1. Shechtman D, Blech I, Gratias D, Cahn JW (1984) Phys Rev Lett 53:1951
2. Inoue A, Bizen Y, Matsumoto T (1988) Metall Trans 19:383
3. Song GS, Fleury E, Kim SH (2002) J Mater Res 17:1671
4. Hippert F, Audier M, Klein H, Bellissent R, Boursier D (1996) Phys Rev Lett 76:54
5. Schenk T, Durand-Charre M, Audier M (1998) J Alloys Comp 281:249
6. Maret M, Lancon F, Billard L (1993) J Phys 3:1873
7. Watanabe M, Inoue A, Kimura HM, Aiba T, Masumoto T (1993) Mater Trans JIM 34:162
8. Inoue A, Kimura HM, Sasamori K, Masumoto T (1996) Mater Trans JIM 37:1287
9. Bouchard R, Hupfeld D, Lippmann T, Neufeind J, Neumann HB, Poulsen HF, Rütt U, Schmidt T, Schneider JR, Süßenbach J, Von Zimmermann M (1998) J Synchrotron Rad 5:90
10. Hammersley AP (1998) ESRF Internal Report, ESRF98HA01T, FIT2D V9.129 Reference Manual V3.1
11. NIST standard reference material, SRM 660a
12. Klementiev KV (2001) J Phys D: Appl Phys 34:209
13. Ankudinov AL, Ravel B, Rehr JJ, Conradson SD (1998) Phys Rev B 58:7565
14. Brandes EA (1983) in Smithells Metals Reference Book, London: Butterworths